

See discussions, stats, and author profiles for this publication at:  
<https://www.researchgate.net/publication/237883262>

# Static inhomogeneity of supercritical ethylene studied by small-angle X-ray scattering

ARTICLE *in* CHEMICAL PHYSICS · JANUARY 2003

Impact Factor: 1.65 · DOI: 10.1016/S0301-0104(02)00935-7

---

CITATIONS

18

---

READS

26

## 4 AUTHORS, INCLUDING:



**Keiko Nishikawa**

Chiba University

217 PUBLICATIONS 3,965 CITATIONS

SEE PROFILE



**Ken-Ichi Saitow**

Hiroshima University

54 PUBLICATIONS 770 CITATIONS

SEE PROFILE



**Takeshi Morita**

Aichi University of Education

12 PUBLICATIONS 185 CITATIONS

SEE PROFILE



# Static inhomogeneity of supercritical ethylene studied by small-angle X-ray scattering

Keiko Nishikawa<sup>\*</sup>, Hiroto Ochiai, Ken-ichi Saitow, Takeshi Morita<sup>1</sup>

*Division of Diversity Science, Graduate School of Science and Technology, Chiba University, Yayoi, Inage-ku, Chiba 263-8522, Japan*

Received 25 February 2002

## Abstract

Small-angle X-ray scattering (SAXS) experiments for supercritical C<sub>2</sub>H<sub>4</sub> were carried out, to study its density fluctuation and correlation length, which are quantitative descriptions of the inhomogeneity of molecular distribution. Except for thermodynamic states near the critical point, the density fluctuation from SAXS experiments is in very good agreement with the one calculated from a new state equation. For investigation on the substance dependence of the inhomogeneity in supercritical states, the results were compared with our previous ones of CO<sub>2</sub>, CF<sub>3</sub>H and H<sub>2</sub>O. The density fluctuation and correlation length for C<sub>2</sub>H<sub>4</sub> show fairly similar behaviors to those of supercritical CO<sub>2</sub>, CF<sub>3</sub>H as a function of reduced density  $\rho_r = \rho/\rho_c$  and reduced temperature  $T_r = T/T_c$ . On the other hand, characteristics for inhomogeneity of supercritical H<sub>2</sub>O are different from those of others. Good correspondence of static inhomogeneity and dynamic one in supercritical C<sub>2</sub>H<sub>4</sub> is revealed, by comparing the fluctuation from SAXS with its correlation time from dynamic light scattering experiments.

© 2002 Elsevier Science B.V. All rights reserved.

## 1. Introduction

The characteristic properties of supercritical fluids are closely related to inhomogeneity of molecular distribution [1]. The inhomogeneity is described in various terms depending on the methodology of investigation and the scale of

observation: for example, formation of clusters with various size, enhancement of local density, and large fluctuation. Clustering is important concept for chemical reactions in supercritical fluids [2], electronic and vibrational energy relaxations of solute molecules in the fluids [2–5], and structure studies from radial distribution functions [6] or computer simulations [7]. From the viewpoint of microscopic inhomogeneity, a great number of spectroscopic studies have been carried out [2] and reviews are presented by combining spectroscopic measurements and computer simulations [3,8]. From the static inhomogeneity in mesoscopic scale, density fluctuation and correlation length are suitable parameters for quantitative

<sup>\*</sup> Corresponding author. Fax: +43-290-3939.

E-mail address: [nisikawa@cuphd.nd.chiba-u.ac.jp](mailto:nisikawa@cuphd.nd.chiba-u.ac.jp) (K. Nishikawa).

<sup>1</sup> Present address: Department of Mechanical Systems Engineering, Faculty of Engineering, Tokyo University of Agriculture and Technology, Naka-cho, Koganei, Tokyo 184-8588, Japan.

description [9,10]. We have comprehensively investigated the density fluctuations at various thermodynamic states of supercritical fluids such as  $\text{CO}_2$  [11,12],  $\text{CF}_3\text{H}$  [13] and  $\text{H}_2\text{O}$  [14] mainly by means of small-angle X-ray scattering (SAXS), and have shown the following facts [9–14]. When the contour map of density fluctuation is drawn in the  $P$ – $T$  phase diagrams, it forms a ridge along the extension of the coexistence curve of gas and liquid. The “ridge” is the locus of the points where the values of the density fluctuation become maximum in isothermal change. The ridge corresponds to maxima or minima of the various physical quantities of supercritical fluids, which are related to the second derivatives of the Gibbs free energy: for example, heat capacity, isothermal compressibility [15], sound velocity [16], thermal conductivity [17] and partial molar volumes [18,19]. From the thermodynamic evidence that the steepest point of the solubility curve corresponds to the minimum of the partial molar volume of solutes at infinite dilution [18,20], the rate of increase in solubility is concluded to become maximum on the ridge [9,10]. In many cases, the rate constants or equilibrium ones of various chemical reactions in supercritical fluids show singular behaviors on the ridge [21–24]. The singularity means maximum, minimum or inflection point of the rate constants, which is dependent on each reaction. The ridge deviates slightly from the critical isochore [25]. The behavior of the correlation length is similar to that of the density fluctuation. All supercritical fluids, to the best of our studies, behave in the same manner for the items mentioned above. These facts show that the density fluctuation and correlation length are important and fundamental parameters for the description of supercritical state.

The next interest is to investigate quantitatively the substance dependence of the behaviors. With reduced density  $\rho_r = \rho/\rho_c$  and reduced temperature  $T_r = T/T_c$ , the contour curves and the ridge drawn in  $\rho_r$ – $T_r$  diagram, and moreover the absolute values for  $\text{CO}_2$  and  $\text{CF}_3\text{H}$  are in agreement with each other [9,10]. The difference, if any, is small. On the other hand, the trends of supercritical  $\text{H}_2\text{O}$  are different from those of  $\text{CO}_2$  and  $\text{CF}_3\text{H}$  [14]. In order to develop the studies on the

substance dependence of the behaviors in density fluctuation and correlation length, we chose supercritical  $\text{C}_2\text{H}_4$ . From the standpoint of inhomogeneity of molecular distribution, no study on supercritical  $\text{C}_2\text{H}_4$  has been reported, as far as we know. Ethylene molecule is one of the typical organic molecules, whose shape is simple and planar. The molecular interaction is characterized by weak quadrupole moment. The first aim of the present study is to compare the behaviors of supercritical  $\text{C}_2\text{H}_4$  to those of  $\text{CO}_2$  [11,12],  $\text{CF}_3\text{H}$  [13] and  $\text{H}_2\text{O}$  [14] and to supply the basic data which will be compared with other supercritical organic compounds such as benzene, cyclohexane and alcohols.

The density fluctuation is also thermodynamically related to isothermal compressibility  $\kappa_T$  [26], by use of which we can calculate the density fluctuation if an accurate equation of state is reported. According to our previous studies for  $\text{CO}_2$ ,  $\text{CF}_3\text{H}$  and  $\text{H}_2\text{O}$ , there is a little difference between the values from SAXS experiments and from thermodynamic calculation. The second aim is to compare to the density fluctuations for supercritical  $\text{C}_2\text{H}_4$  obtained from the two methods.

The third aim is to give the structural data for supercritical  $\text{C}_2\text{H}_4$  from the viewpoint of static inhomogeneity, and to compare it with the dynamic inhomogeneity obtained from the dynamic light scattering (DLS) experiment [27] and so on. We are interested in how the inhomogeneity is observed dependent on the methodology or the observation scale. For supercritical  $\text{CO}_2$ , the density dependence of the width of a vibrational band from Raman scattering [28] corresponds well to the behavior of the density fluctuation from SAXS [9–12]. This will show that the band width is significantly related to the inhomogeneous surroundings of the molecule, which will just refer to the static inhomogeneity from SAXS. For supercritical  $\text{CF}_3\text{H}$ , on the other hand, the enhancement of local density estimated from the vibrational modes of Raman spectra shows slightly different behavior [29] from the SAXS results [9,10,13]. For supercritical  $\text{CF}_3\text{H}$ , the rotational and hindered librational motions obtained from far infrared absorption spectra using THz radiation are discussed in relation to the static inhomogeneity by

the SAXS data [30]. We are also investigating the behavior of inhomogeneity for supercritical  $\text{C}_2\text{H}_4$  by various methods. The present results by SAXS supply the data as static and mesoscopic inhomogeneity. In the present paper, these are compared with our recent results on correlation time of diffusive motion of aggregates as dynamic inhomogeneity [27].

## 2. Experimental section

Scattering measurements for supercritical  $\text{C}_2\text{H}_4$  were carried out at BL-15 station, Photon Factory (PF) at National Laboratory for High Energy Accelerator Research Organization (KEK), Tsukuba, by use of the SAXS apparatus settled at the station [31,32]. By a bent mirror and a bent monochromator made of Si single crystal, X-ray of 1.50 Å in wavelength was selected and the beam was focused to  $1 \times 1 \text{ mm}^2$  at a position sensitive proportional counter. The camera length was set in 2000 mm, and the X-ray path was evacuated except the position where the sample holder was set. The observable  $s$ -region in the present measurements was  $0.015\text{--}0.18 \text{ Å}^{-1}$ , where the scattering parameter  $s$  is defined as  $4\pi \sin \theta / \lambda$  ( $2\theta$ : scattering angle,  $\lambda$ : wavelength of X-ray). The experimental procedures in the present study were the same as those of our previous experiments for supercritical  $\text{CO}_2$  [11,12] and  $\text{CF}_3\text{H}$  [13].

The present sample holder was the same type as the one reported previously [13], which consisted of the body made of SUS316 and the windows of diamond disks of 4 mm in diameter and 0.4 mm in thickness. The sample length was about 2 mm. The temperature of the sample was kept constant by flowing temperature-controlled water through a jacket of the sample holder. A thermocouple and a strain gauge being directly immersed in the sample, temperature and pressure were monitored at very near the position where X-rays were scattered.

The used values for critical constants of  $\text{C}_2\text{H}_4$  are  $T_c = 282.4 \text{ K}$ ,  $P_c = 5.04 \text{ MPa}$  and  $\rho_c = 0.214 \text{ g cm}^{-3}$ . The SAXS intensities were measured along the three isotherms at the temperatures of 288.1, 293.7 and 299.3 K, which correspond to 1.021, 1.04 and 1.06 in reduced

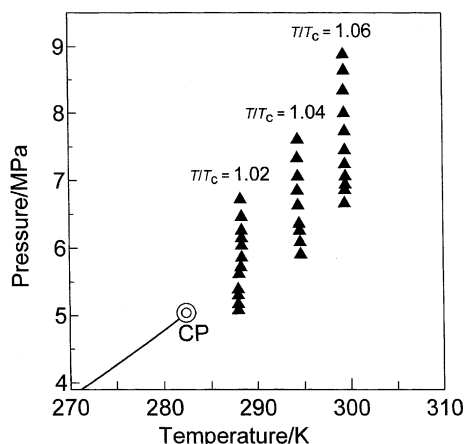


Fig. 1. Measured thermodynamic states of supercritical  $\text{C}_2\text{H}_4$  drawn on a pressure–temperature phase diagram. The solid line refers to the gas–liquid coexistence curve and CP means the critical point.

temperature  $T_r$  defined by  $T/T_c$ . The pressure was varied in the range of 5.0–9.0 MPa. The densities were calculated from the state equation for  $\text{C}_2\text{H}_4$  [33] by use of measured temperature and pressure. Fig. 1 shows the measurement points in a  $P$ – $T$  diagram. The accumulation time for an intensity measurement of each sample was 600 s. During a measurement, the pressure and the temperature were kept constant within the range of 0.01 MPa and 0.1 K, respectively. There is no leakage of the sample during each measurement. The fluctuations of the pressure were due to the temperature deviation of the sample. Various corrections for the observed scattering intensities were made, i.e., the subtraction of instrumental backgrounds, the absorption correction, and the correction for the fluctuation of the beam intensity.

## 3. Results and discussion

According to the Ornstein–Zernike theory, the small-angle scattering intensity of a sample near the critical point is given by [26]

$$I(s) = \frac{I(0)}{1 + \xi^2 s^2}, \quad (1)$$

where  $\xi$  is the Ornstein–Zernike correlation length and  $I(0)$  is the scattering intensity at  $s = 0$  (zero-

angle scattering intensity). If the Ornstein–Zernike regime is operative, the Ornstein–Zernike plot of  $1/I(s)$  vs.  $s^2$  forms a straight line. The correlation length is evaluated from the slop of the line.

The procedure to obtain density fluctuation is as follows. For  $N$  molecules in arbitrary volume  $V$ , the fluctuation  $\langle(\Delta N)^2\rangle$  is represented by

$$\langle(\Delta N)^2\rangle = \langle(N - \overline{N})^2\rangle, \quad (2)$$

where  $\langle \rangle$  or overline means the averaged value. Since the fluctuation given by Eq. (2) depends on

the size of  $V$ , the density fluctuation is defined by  $\langle(\Delta N)^2\rangle/\overline{N}$  as an intensive variable, and it is related to zero-angle X-ray scattering intensity  $I(0)$  as follows [26]:

$$\frac{\langle(\Delta N)^2\rangle}{\overline{N}} = \frac{1}{Z^2} \frac{I(0)}{N}, \quad (3)$$

where  $Z$  is the number of electrons in a molecule. Since the  $I(0)$  value from the extrapolation in the Ornstein–Zernike plot is in arbitrary unit, it is necessary to estimate the  $I(0)$  value per molecule.

Table 1  
Correlation length and density fluctuation of supercritical C<sub>2</sub>H<sub>4</sub>

$T$ (K)	$P$ (MPa)	$\rho^a$ (g cm <sup>-3</sup> )	$\xi$ (Å)	$\langle(\Delta N)^2\rangle/N$
$T/T_c = 1.02$				
288.0	5.08	0.115	9.0	5.9
288.0	5.17	0.122	9.9	7.0
288.0	5.30	0.134	11.6	9.4
288.0	5.39	0.144	13.8	12.9
288.1	5.62	0.188	20.1	28.0
288.3	5.72	0.213	17.2	17.6
288.4	5.86	0.246	14.2	10.3
288.4	6.04	0.271	11.6	6.0
288.4	6.15	0.280	10.5	4.7
288.4	6.26	0.288	9.6	3.9
288.4	6.46	0.299	8.6	3.0
288.3	6.72	0.310	7.7	2.3
$T/T_c = 1.04$				
294.7	5.91	0.147	9.4	7.5
294.7	6.09	0.165	11.1	9.7
294.6	6.26	0.187	12.8	12.0
294.6	6.36	0.202	13.3	12.3
294.5	6.63	0.238	12.4	10.4
294.4	6.85	0.259	11.1	7.4
294.5	7.06	0.272	9.9	5.3
294.4	7.33	0.286	8.7	3.8
294.5	7.61	0.297	7.8	3.0
$T/T_c = 1.06$				
299.5	6.66	0.180	10.1	7.9
299.5	6.86	0.198	10.8	8.5
299.6	6.94	0.205	10.9	8.5
299.6	7.06	0.216	10.9	8.2
299.5	7.24	0.232	10.7	7.3
299.5	7.45	0.247	10.0	6.0
299.5	7.73	0.263	9.1	4.7
299.5	8.00	0.276	8.4	3.8
299.4	8.34	0.289	7.6	2.9
299.5	8.64	0.297	7.0	2.5
299.4	8.88	0.304	6.6	2.2

<sup>a</sup> Densities are calculated by using the equation of state for C<sub>2</sub>H<sub>4</sub> from [33].

The density fluctuation is also related to the isothermal compressibility  $\kappa_T$  by the following equation [26]:

$$\frac{\langle(\Delta N)^2\rangle}{N} = \rho \kappa_T k_B T, \quad (4)$$

where  $k_B$  is the Boltzmann constant,  $\rho$  is the number density, and  $\kappa_T$  is defined by

$$\kappa_T = -\frac{1}{V} \left( \frac{\partial V}{\partial P} \right)_T = \frac{1}{\rho} \left( \frac{\partial \rho}{\partial P} \right)_T. \quad (5)$$

Namely, the density fluctuation is thermodynamically estimated from numerical differential of the  $\rho$  and  $P$  ensembles calculated from the empirical state equation. The scaling factor to normalize the experimental X-ray scattering intensity to absolute scale is determined by comparison of the thermodynamic data for the states far from the critical density and critical temperature, the reason of which will be discussed later. In this way, the density fluctuation is evaluated from SAXS experiments. The Ornstein–Zernike plots for all the present data of supercritical  $C_2H_4$  formed straight lines. Although it is well known that the plot deviates slightly from the straight line in the extreme vicinity of the critical temperature [34],  $T_r$  is larger than 1.02 in the present study, which is far from the critical temperature enough for the Ornstein–Zernike theory to be applicable. As the state equation to normalize SAXS intensities, we applied the one recently reported by Smukala et al. [33]. The determined values for density fluctuation and correlation length are listed in Table 1.

The isothermal changes of density fluctuation against density are shown by triangles at  $T_r = 1.021$ , 1.04, 1.06 in Fig. 2. For comparison, the ones calculated from the state equation by Smukala et al. [33] and by Younglove [35] are also shown by solid curves and broken curves, respectively. Although the densities calculated from the two state equations agree well with each other within the deviation of 0.1%, the density fluctuations fairly differ; the difference becomes conspicuous as the density and temperature approach critical values. This will be because the density fluctuation from thermodynamic data is a differential value of density. A very little deviation in the values of density will cause a fairly large deviation

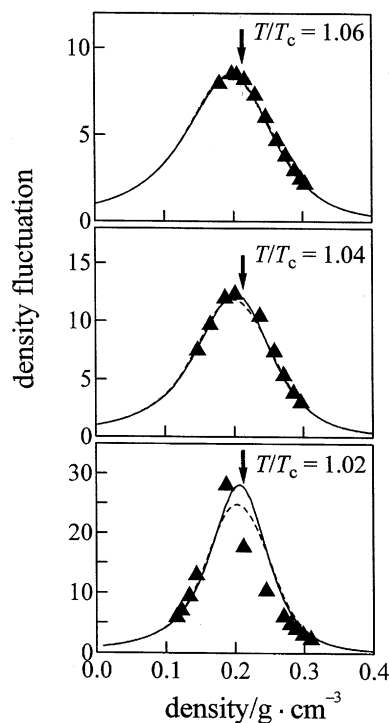


Fig. 2. Comparison of density fluctuations for supercritical  $C_2H_4$  obtained from present SAXS experiments ( $\blacktriangle$ ) and thermodynamic calculation using the empirical state equations by Smukala et al. [33] (solid curves) and by Younglove [35] (broken curves). The arrows show the critical density.

by taking a differential procedure. Except for the isotherm of  $T_r = 1.021$ , the agreement between the values from SAXS and from the two state equation [33,35] is very good. For the differences in the isotherm of  $T_r = 1.021$ , we can point out the following possibilities; the difference in the scale of observation, the accuracy of our SAXS experiment, and the accuracy of the state equation. First, we discuss a problem of the scale of observation. The empirical state equation is obtained by function fitting for a great number of  $P$ – $\rho$ – $T$  data. So, the density fluctuation calculated from the state equation is, of course, macroscopic average; namely the volume  $V$  mentioned in the explanation of Eq. (2) is macroscopic scale. In X-ray scattering experiment, the scale of the observation is regarded as the coherent length of the X-ray, which is estimated to be the order of  $10^4$  Å, namely mesoscopic scale. The observation scale is dis-

cussed by Okazaki et al. [36], defining the following parameter:

$$\alpha(r) = \left( \frac{\langle (\Delta N)^2 \rangle}{\bar{N}} \right)_r \bigg/ \left( \frac{\langle (\Delta N)^2 \rangle}{\bar{N}} \right)_\infty = \left( 1 + 4\pi\rho \int_0^r R^2 [G^N(R) - 1] dR \right) / S(0), \quad (6)$$

where the suffixes  $r$  and  $\infty$  stand for the observation scales and  $S(s)$  and  $G^N(R)$  are structure factor and radial distribution function from neutron scattering experiments. By use of their wide- and small-angle neutron scattering data, they obtained  $\alpha$  values for some thermodynamic states of supercritical  $\text{CO}_2$ . According to their analysis, the difference between local (finite region defined by  $r$ ) and bulk (thermodynamic infinity) density fluctuations becomes smaller as the scale  $r$  becomes larger, and the difference is about 25% at 30 Å [36,37]. This means that the magnitude of density fluctuation approaches asymptotically the thermodynamic limit as increase of the scale. Since the probed scale of the SAXS experiment is much longer than a few tens of Å, it is safely described that the density fluctuation from the SAXS reaches to the thermodynamic one. Namely, the fluctuation determined by SAXS experiment and by the thermodynamic calculation should be in agreement with each other, if there is little error in the experiments and the empirical state equation is correct enough to discuss differentiated valuables. There will be, of course, some experimental errors in the SAXS data, especially in the data as approaching to the critical point because it is hard to hold steadily the sample at a determined thermodynamic state. The differences are, however, observed characteristically in the neighborhood of the critical density or the ridge (Fig. 2). The thermodynamic fluctuation is obtained by numerical differential of the  $\rho$  and  $P$  ensembles from the empirical state equation as shown in Eq. (5). On the other hand, the SAXS fluctuation is determined from the directly measurable  $I(0)$  value. Much error is apt to be introduced when taking differential, especially in the points where variables are changing anomalously. We have pointed out that the ridge is a locus of extremes of variables

which relate to the second derivatives of the Gibbs free energy. In our previous paper, it is presented that the ridge is the trace of the first-order phase transition of gas and liquid and may be a locus of higher order phase change [10,13]. It will be impossible to express such anomaly by a simple state equation.

Since the anomaly appears only in the neighborhood of the ridge and the observation scale of SAXS experiments is large enough to regard that the values of density fluctuation reach the thermodynamic limit, it is safely permitted to make scaling of SAXS intensity data by the thermodynamic parameter if the data for the thermodynamic states far from the ridge are compared.

The density fluctuation is the quantitative description of the inhomogeneity in the distribution of molecules. The isothermal changes of the values for supercritical  $\text{C}_2\text{H}_4$  are shown at  $T_r = 1.021$ , 1.04, 1.06 in Fig. 3, with the results of  $\text{CO}_2$  [12] and  $\text{CF}_3\text{H}$  [13]. Temperature and density are described

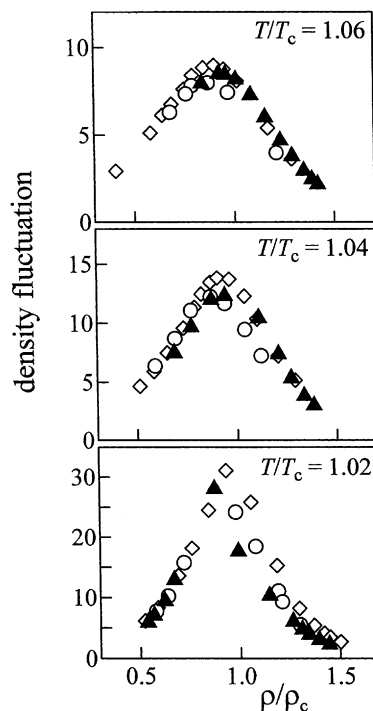


Fig. 3. Comparison of density fluctuations among  $\text{C}_2\text{H}_4$  (▲),  $\text{CO}_2$  (○) and  $\text{CF}_3\text{H}$  (◇).

as the reduced values which are normalized ones by the respective critical constants. Two conclusions are led from Fig. 3. First, the characteristic in the isothermal change of the values for supercritical  $\text{C}_2\text{H}_4$  is in good agreement with those of  $\text{CO}_2$  and  $\text{CF}_3\text{H}$  within experimental errors and difference of temperature setting. Second, the maxima of the density fluctuation deviate from the critical density ( $\rho_r = 1.0$ ), and the deviation becomes larger as temperature is far from the critical temperature. These behaviors are observed for all the samples which we have studied [9–14]. We defined the ridge of the density fluctuation as the locus of the maxima in isothermal changes [9–11]. We have proposed that the ridge is the boundary which divides the supercritical region into liquid-like and gas-like regions, from the SAXS results [10] and the Raman scattering measurements [28]. The ridge being the boundary, drastically change the properties of the supercritical fluids as mediums for reaction and extraction. Therefore, for discussion on the properties of supercritical fluids, it is important to know how the ridge is in the phase diagram. The agreement of the maxima for the samples proves that the ridges overlap with each other in  $\rho_r$ – $T_r$  phase diagram.

Near the critical point, the correlation length  $\xi$  is related to the pair correlation function  $g(r)$  by the following equation [26]:

$$g(r) - 1 = \frac{k_B T \kappa_T \exp(-r/\xi)}{4\pi \xi^2 r}. \quad (7)$$

Eq. (7) indicates that the envelop of a pair correlation function decreases exponentially and correlation length  $\xi$  is the parameter of the decrease. Namely, in supercritical fluids, the distribution of molecular aggregation number is represented with exponential decay, so that the structure cannot be discussed by a simple cluster size. The correlation length is the measure of the inhomogeneity of molecular distribution from the viewpoint on dimension of length. The isothermal changes of correlation length for  $\text{C}_2\text{H}_4$  are shown in Fig. 4 as a function of density. For comparison, those for  $\text{CO}_2$  and  $\text{CF}_3\text{H}$  are also plotted in the same figure. As well as the density fluctuation, the values of the correlation length for three substances agrees well with each other, and the maxima shift slightly to

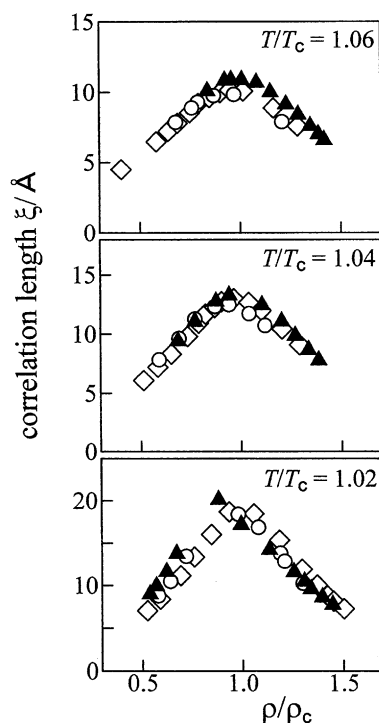


Fig. 4. Comparison of correlation lengths among  $\text{C}_2\text{H}_4$  (▲),  $\text{CO}_2$  (○) and  $\text{CF}_3\text{H}$  (◇).

lower densities than the critical one. The maxima for the correlation length refer to those for the density fluctuation.

It is proved that the behaviors and absolute values of the density fluctuation of supercritical  $\text{C}_2\text{H}_4$  are in good correspondence with those of  $\text{CO}_2$  and  $\text{CF}_3\text{H}$ . The molecular interaction of  $\text{C}_2\text{H}_4$  is characterized by weak quadrupole moment,  $\text{CO}_2$  by strong quadrupole one, and  $\text{CF}_3\text{H}$  by strong dipole one. The shapes of the molecules are quite different. The good agreement in the density fluctuation shows that it is one of the universal variable independent of substances; namely the law of corresponding states [26] is operative. The above-mentioned conclusion is also speculated from the facts that the density fluctuation is a dimensionless variable. As shown in our previous paper for supercritical  $\text{H}_2\text{O}$  [14], the behaviors of  $\text{H}_2\text{O}$  are different from others. The molecules with hydrogen bonding will be the exception of the law of corresponding states.



For the behaviors of the correlation length as a function of  $\rho_r$  and  $T_r$ , the good similarity in  $C_2H_4$ ,  $CO_2$  and  $CF_3H$  are also observed. This result will be natural, because molecular sizes of the present three samples are not so different. The correlation lengths of  $H_2O$  are, as a whole, smaller than those of the three samples, while the values of density fluctuation of  $H_2O$  are larger [14]. The preliminary study on supercritical  $C_6H_6$  with larger molecular size shows longer correlation length [38]. These results suggest that correlation length should be normalized by respective molecular size for discussion on the correspondence of the length. This procedure, which makes the variable dimensionless, will be reasonable. The comprehensive studies are the future theme how the molecular size and molecular interaction affect the behaviors of the correlation length.

We are also interested in the dynamics of inhomogeneity and have carried out dynamic light scattering (DLS) experiments of supercritical  $C_2H_4$  at the same isotherms as the present SAXS experiments [27]. Light intensity correlation functions for all the thermodynamic states decay as single exponential functions with the time constant of order of 1  $\mu s$ . With correlation time  $\tau$ , the electric field correlation function is described by

$$E^*(t)E(0) \propto \exp(-t/\tau), \quad (8)$$

where  $E^*(t)$  is complex conjugate of electric field  $E(t)$ . The  $\tau$  values for  $2\theta = 30^\circ$  ( $s = 6.7 \times 10^{-3} \text{ nm}^{-1}$ ) are shown by circles in Fig. 5, with the density fluctuation by triangles. The density dependence of the correlation time shows the similar curves with that of the static density fluctuation.

The matter to be discussed is the observation scales in time and space. In the DLS experiments, the sampling time was 200 ns. Namely, we observe not the fast motions of individual molecules in ps order but the time evolution of the motions of the clusters in the whole observed space. Moreover, time correlation function was space-averaged in the experiment. The spatial scale of observation referred to the coherent length of the used laser or the volume contributing the scattering; in any case, macroscopic spatial average was carried out. From the facts mentioned above, the correlation time in our DLS experiments is the one for diffusive mo-

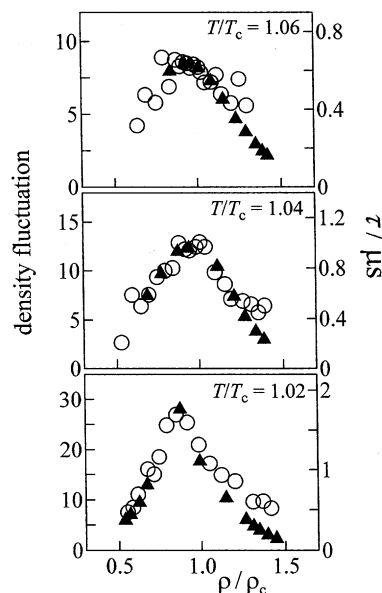


Fig. 5. Correspondence between density fluctuation ( $\blacktriangle$ ) by SAXS and correlation time of density fluctuation ( $\circ$ ) by DLS.

tion of clusters with various sizes, which repeat appearance and disappearance in ultra-fast time scale. Though the sampling time and spatial observation scale are different with each other in the SAXS experiments and DLS ones, it is safely said that the observation scales of the both methods reach the thermodynamic limit. Therefore, it can be said that the correlation time measured DLS corresponds to the dynamic information of the static fluctuation obtained by SAXS.

As shown in Fig. 5, the density dependence of correlation time  $\tau$  and density fluctuation show the similar isotherms. As the wavelength of the used  $Ar^+$  laser in the DLS experiments was 448 nm and it is much longer than the correlation length  $\xi$  of the sample,  $\tau$  is related to [26]

$$\tau = 1/(D_T s^2) = \rho C_p / \Lambda s^2, \quad (9)$$

where  $D_T$  is the thermal diffusivity,  $\Lambda$  is the thermal conductivity,  $\rho$  is the density, and  $C_p$  is the specific heat capacity at constant pressure. As thermal conductivity  $\Lambda$  is almost proportional to the density except for the thermodynamic state extremely close to the critical point [17,39],  $\rho/\Lambda$  in Eq. (9) becomes almost constant and we obtain the following relation:

$$\tau \propto C_p. \quad (10)$$

Density fluctuation  $\langle(\Delta N)^2\rangle/N$  and specific heat capacity  $C_p$  are the representative variables of the second derivatives of the Gibbs free energy [40]. As mentioned in Section 1, the variables, which are related to the second derivatives of the Gibbs free energy, behave in the similar manner; especially the variables have extremes on the ridge of density fluctuation. As given by Eq. (10), the value of  $\tau$  is related  $C_p$  and in turn density fluctuation.

The correlation time becomes maximum just on the ridge of the density fluctuation; namely the slowing-down of the diffusive motions of  $C_2H_4$  clusters occurs on the thermodynamic state at which the molecular distribution is most disordered in an isothermal change. The combination of the present SAXS and the DLS experiments is the first report of the inhomogeneity of molecular distribution in supercritical state from the static and dynamic viewpoints, and shows the good correspondence of static and dynamic behaviors. The results from the DLS experiment have been discussed in detail from the point of view on dynamics of molecules [27].

## Acknowledgements

The authors wish to express their thanks to PF at KEK for giving them the opportunity to perform the SAXS experiments. This work was supported in part by a Grant-in-Aid for Scientific Research from the Ministry of Education, Science and Culture, Japan.

## References

- [1] For example: E. Kiran (Ed.), Proceedings of the 4th International Symposium on Supercritical Fluids, Special Issue J. Supercritical Fluids 13 (1998).
- [2] O. Kajimoto, Chem. Rev. 99 (1999) 355, and references therein..
- [3] S.C. Tucker, Chem. Rev. 99 (1999) 391, and references therein..
- [4] For example: S.A. Egorov, J.L. Skinner, J. Phys. Chem. A 104 (2000) 483.
- [5] For example: D.J. Myers, M. Shigeiwa, M.D. Fayer, B.J. Cherayil, J. Phys. Chem. B 104 (2000) 2402.
- [6] For examples: P. Postorino, R.H. Tromp, M.A. Ricci, A.K. Soper, G.W. Neilson, Nature 366 (1993) 668; K. Yamanaka, T. Yamaguchi, H.J. Wakita, Chem. Phys. 101 (1994) 9830; A.K. Soper, F. Bruni, M.A. Ricci, J. Chem. Phys. 106 (1997) 247; T. Morita, K. Nishikawa, M. Takematsu, H. Iida, S. Furutake, J. Phys. Chem. B 101 (1997) 7158.
- [7] For examples: I.B. Petsche, P.G. Debenedetti, J. Chem. Phys. 91 (1989) 7075; S. Okazaki, M. Matsumoto, I. Okada, K. Maeda, Y. Kataoka, J. Chem. Phys. 103 (1995) 8594; P. Jedlovsky, J.P. Brodholt, F. Bruni, M.A. Ricci, A.K. Soper, R. Vallauri, J. Chem. Phys. 108 (1998) 8528.
- [8] S.C. Tucker, M.W. Maddox, J. Phys. Chem. B 102 (1998) 2437, and references therein..
- [9] K. Nishikawa, T. Morita, J. Supercritical Fluids 13 (1998) 143.
- [10] K. Nishikawa, T. Morita, Chem. Phys. Lett. 316 (2000) 238.
- [11] K. Nishikawa, I. Tanaka, Chem. Phys. Lett. 244 (1995) 149.
- [12] K. Nishikawa, I. Tanaka, Y. Amemiya, J. Phys. Chem. 100 (1996) 418.
- [13] K. Nishikawa, T. Morita, J. Phys. Chem. B 101 (1997) 1413.
- [14] T. Morita, K. Kusano, H. Ochiai, K. Saitow, K. Nishikawa, J. Chem. Phys. 112 (2000) 4203.
- [15] M. Kamiya, K. Muroki, M. Uematsu, J. Chem. Thermodynamics 27 (1995) 337.
- [16] E.F. Carome, C.B. Cykowski, J.F. Havlice, D.A. Swyt, Physica 38 (1968) 307.
- [17] Z. Chen, K. Tozaki, K. Nishikawa, Jpn. J. Appl. Phys. 38 (1999) 6840.
- [18] C.A. Eckert, D.H. Ziger, K.P. Johnston, S.J. Kim, Phys. Chem. 90 (1986) 2738.
- [19] C.A. Eckert, B.L. Knutson, P.G.. Debenedetti, Nature 383 (1996) 313.
- [20] R.T. Kurnik, R.C. Reid, AIChE J. 27 (1981) 861.
- [21] B. Otto, J. Schroeder, J. Troe, J. Chem. Phys. 81 (1984) 202.
- [22] G.M. Simmons, D.M. Mason, Chem. Eng. Sci. 27 (1972) 89.
- [23] Y. Kimura, Y. Yoshimura, J. Chem. Phys. 96 (1992) 3824.
- [24] Y. Ikushima, N. Saito, M. Arai, J. Phys. Chem. 96 (1992) 2293.
- [25] C.G. Gray, S. Goldman, B. Tomberli, W. Li, Chem. Phys. Lett. 271 (1997) 185.
- [26] H.E. Stanley, Introduction to Phase Transitions and Critical Phenomena, Oxford University Press, Oxford, 1971.
- [27] K. Saitow, H. Ochiai, T. Kato, K. Nishikawa, J. Chem. Phys. 116 (2002) 4286.
- [28] H. Nakayama, K. Saitow, M. Sakashita, K. Ishii, K. Nishikawa, Chem. Phys. Lett. 320 (2000) 323.
- [29] K. Saitow, K. Ohtake, H. Nakayama,, K. Ishii, K. Nishikawa, Chem. Phys. Lett. (in press).

- [30] K. Saitow, H. Ohtake, N. Sarukura, K. Nishikawa, *Chem. Phys. Lett.* 341 (2001) 86.
- [31] Y. Amemiya, K. Wakabayashi, T. Hamanaka, T. Wakabayashi, T. Matsushita, H. Hashizume, *Nucl. Instr. Methods* 208 (1983) 471.
- [32] K. Wakabayashi, Y. Amemiya, in: S. Ebashi, M. Koch, E. Rubinstein (Eds.), *Handbook on Synchrotron Radiation*, vol. 4, North-Holland, Amsterdam, 1991 (Chapter 19).
- [33] J. Smukala, R. Span, W. Wagner, *J. Phys. Chem. Ref. Data* 29 (2000) 1053.
- [34] M.E. Fisher, *J. Math. Phys.* 5 (1964) 944.
- [35] B.A. Younglove, *J. Phys. Chem. Ref. Data* 11 (Suppl.) (1982) 1.
- [36] R. Ishii, S. Okazaki, I. Okada, M. Furusaka, N. Watanabe, M. Misawa, T. Fukunaga, *Chem. Phys. Lett.* 240 (1995) 84.
- [37] R. Ishii, S. Okazaki, I. Okada, M. Furusaka, N. Watanabe, M. Misawa, T. Fukunaga, *J. Chem. Phys.* 105 (1996) 84.
- [38] A. Ayusawa, T. Morita, K. Nishikawa, *J. Chem. Phys.* (in preparation).
- [39] A. Michels, J.V. Sengers, *Physica* 28 (1962) 1238.
- [40] Y. Koga, *J. Phys. Chem.* 100 (1996) 5172.